Journal of Microscopy, Vol. 194, Pt 2/3, May/June 1999, pp. 477–482.
Received 6 December 1998; accepted 30 January 1999

Single molecule mapping of the optical field distribution of probes for near-field microscopy

J. A. VEERMAN, M. F. GARCIA-PARAJO, L. KUIPERS & N. F. VAN HULST
Applied Optics Group, Faculty of Applied Physics & MESA$^+$ Research Institute, University of Twente, PO Box 217, 7500 AE Enschede, The Netherlands

Key words. Fluorescence microscopy, focused ion beam, near-field scanning optical microscopy, shear force microscopy, single molecule detection.

Summary

The most difficult task in near-field scanning optical microscopy (NSOM) is to make a high quality subwavelength aperture probe. Recently, we have developed high definition NSOM probes by focused ion beam (FIB) milling. These probes have a higher brightness, better polarization characteristics, better aperture definition and a flatter end face than conventional NSOM probes. We have determined the quality of these probes in four independent ways: by FIB imaging and by shear-force microscopy (both providing geometrical information), by far-field optical measurements (yielding throughput and polarization characteristics), and ultimately by single molecule imaging in the near-field. In this paper, we report on a new method using shear-force microscopy to study the size of the aperture and the end face of the probe (with a roughness smaller than 1·5 nm). More importantly, we demonstrate the use of single molecules to measure the full three-dimensional optical near-field distribution of the probe with molecular spatial resolution. The single molecule images exhibit various intensity patterns, varying from circular and elliptical to double arc and ring structures, which depend on the orientation of the molecules with respect to the probe. The optical resolution in the measurements is not determined by the size of the aperture, but by the high optical field gradients at the rims of the aperture. With a 70 nm aperture probe, we obtain fluorescence field patterns with 45 nm FWHM. Clearly, this unprecedented near-field optical resolution constitutes an order of magnitude improvement over far-field methods like confocal microscopy.

Focused ion beam etching of NSOM probes

Major improvements in the optical characteristics of aluminium coated NSOM fibre probes have been accomplished by side-on milling with a focused ion beam (Veerman *et al.*, 1998). This treatment produces a flat-end face free of aluminium grains with a well-defined circularly symmetric aperture. The size of the aperture can be set in a controlled way down to 20 nm. The polarization behaviour of the probes is circularly symmetric with a polarization ratio exceeding 1 : 100. Single molecule fluorescence signals increase more than one order of magnitude over unmodified probes with the same aperture. With the new probes we could increase the time resolution for monitoring single molecule fluorescence to 30 μs. For the first time, we have observed real time intersystem crossing of single molecules to the triplet state with NSOM (results will be published elsewhere).

A high-resolution image of the probe can be made with the FIB apparatus by detecting secondary electrons that are generated while scanning the ion beam. In this way, the size of the aperture and the thickness of the coating can be determined with an accuracy of 5 nm (Veerman *et al.*, 1998). Figure 1 shows two images of FIB-etched probes with apertures of 70 (± 5) nm (a) and 45 (± 5) nm diameter (b). Note the well-defined circularly symmetric apertures, the flat end face and the smooth aluminium coating.

Shear-force microscopy

The ideal aperture NSOM probe should have a perfectly flat end face to position a sample as close as possible into the near-field of the aperture. Conventional probes generally have a roughness determined by the grain size of the aluminium coating, which is ≈ 20 nm at best (Hollars & Dunn, 1998). Due to the corrugated end face the distance between aperture and sample increases, which lowers the optical resolution and decreases the light intensity on the sample. Furthermore, these grains often obscure the aperture, which makes the probe ill-defined and not suited for quantitative measurements.

Correspondence to: J. A. Veerman. Tel: + 31 53 489 4002; fax: + 31 53 489 1105. e-mail: j.a.veerman@utwente.nl

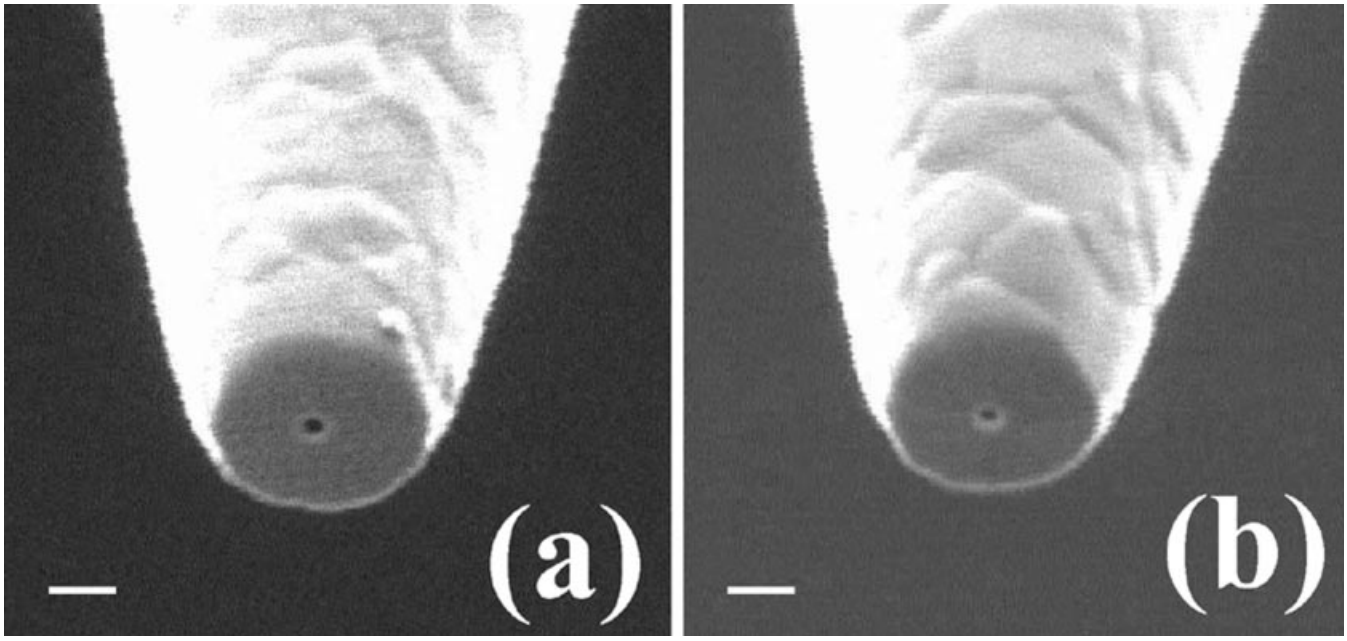

Fig. 1. FIB images of FIB-etched NSOM probes with aperture diameters of (a) 70 (± 5) nm and (b) 45 (± 5) nm. The probes have a flat end face and the apertures have well-defined edges and are circularly symmetric. Bar = 200 nm.

The roughness of the end face of our FIB-etched probes is lower than the resolution limit of the FIB machine (≈ 5 nm). An adequate measure of the roughness would require a high resolution scanning probe method. However, scanning the end face of the probe with an AFM or STM is hardly possible in practice. Thus, we have performed the measurement in an alternative way. Usually, a NSOM probe is scanned over a surface using shear-force feedback as a distance regulation mechanism. We use tuning-fork shear-force microscopy (Karrai & Grober, 1995) with a height resolution better than 0·1 nm (Ruiter *et al.*, 1997a). We have scanned a 100-nm aperture FIB-modified NSOM probe in tuning-fork shear-force feedback over an extremely flat polymer thin film with some dispersed small protrusions. A height image is shown in Fig. 2(a). In general, resolution in a scanning probe height image is always a convolution of probe shape and sample topography. In this case, the small protrusions of the sample are much smaller than the probe size. This implies that the protrusions effectively act as sharp 'sample' probes that map the end face of the NSOM probe (Fig. 2(b)). As a result, both discs in the right part of Fig. 2(a) represent the end face of the NSOM probe. The RMS roughness of the end face is less than 1·5 nm as deduced from this image. Two small particles sticking to the probe and a slightly depressed region at the side of the end face are also visible.

In the middle of the discs a darker region of 100 (± 5) nm diameter is visible that represents the aperture. In this way, the aperture size can be checked independently from the FIB images. Both values are in excellent agreement. The presence of contrast suggests that the aperture is slightly depressed (≈ 2 nm) with respect to the outer part of the end face. Although FIB milling is known to be highly anisotropic independent of the material, we cannot exclude the milling as a cause for the observed height difference. However, it may well be that the contrast in the image is not only due to a height difference, but also due to the material difference between coating (aluminium) and aperture (silica). It is known (Ruiter *et al.*, 1997a) that the shear-force damping mechanism is sensitive to sample properties, i.e. the hydrophobicity of the surface.

Single molecule measurements

The best way to obtain detailed information about the optical near-field distribution of the aperture of a NSOM probe is to use a single fluorescent molecule as a local detector (Betzig & Chichester, 1993; Veerman *et al.*, 1998). A fluorescent molecule will only be excited if the polarization of the optical electric field is parallel to its absorption dipole moment. By moving a fluorescent molecule with a fixed orientation in the near-field of the NSOM probe, the electric field components in that particular direction are mapped with subnanometre accuracy (determined by the absorption cross-section of the molecule).

We have measured the three-dimensional optical near-field distribution of our FIB-modified NSOM probes for different polarization states. Experimental details of the set-up have been described elsewhere (Ruiter *et al.*, 1997b). Figure 3 shows a NSOM fluorescence image of several hundred spatially dispersed randomly distributed $DiIC_{18}$

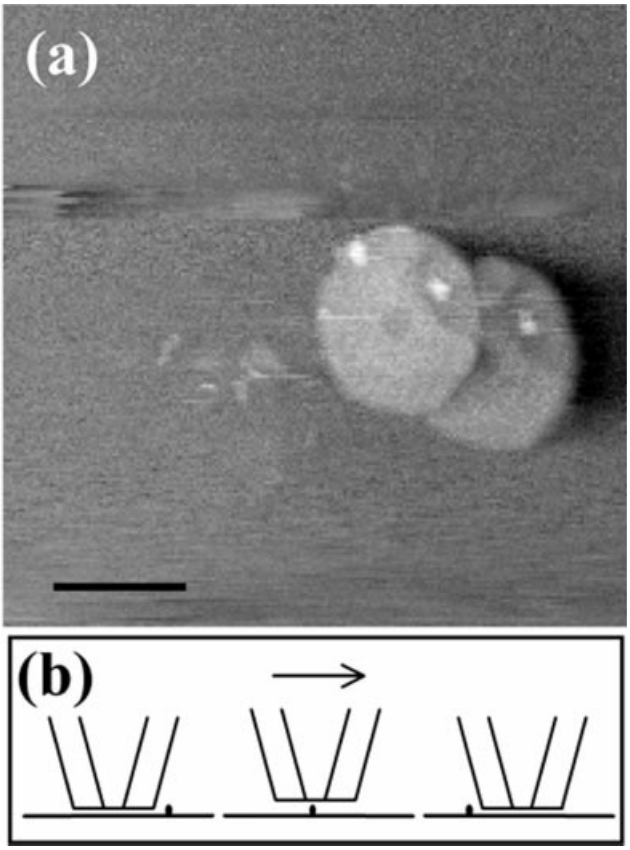

Fig. 2. (a) Shear-force height image ($2{\cdot}4 \times 2{\cdot}4\ \mu$m) of a thin film of PMMA, obtained by scanning a 100 nm NSOM probe in shear-force feedback over the surface. The two discs are height maps of the end face of the probe induced by small protrusions of the surface, as illustrated in (b). The small dark centre of the discs represents the aperture of the probe. The image provides an independent measure of the aperture size and the roughness of the probe, which is less than 1·5 nm. Bar = 500 nm.

molecules. We used the 70 nm aperture probe of Fig. 1(a) emitting circularly polarised light (measured in the far-field) for this measurement. Due to the small aperture size of the probe it was possible to detect each molecule individually. In contrast, the optical resolution of far-field methods (like confocal or wide-field microscopy) would be too large to spatially separate molecules in this sample. A false colour scale is applied in the image that represents the polarization of the detected light, and thus the in-plane orientation of the emission dipole moment of the molecules (Ruiter *et al.*, 1997b). Both 'green' molecules (in-plane orientation in the vertical image direction), 'red' molecules (horizontal image direction) and 'yellow' molecules (orientated in between) are visible. Most important to note are the different shapes of the single molecule spots in the image. Some molecules appear as circular dots, while others look like symmetric or asymmetric rings. This means that a molecule undergoes selective excitation as a function of its position with respect to the probe, and that this function changes from molecule to molecule. In fact, this function is dependent on the orientation of the molecule, because only when the polarization of the optical field is parallel to the absorption dipole moment of a molecule, it will be excited. As the molecules in the PMMA thin film have randomly distributed orientations, all polarization components of the probe can be measured this way.

Over 50 years ago, analytical expressions for the electric field distribution in a subwavelength aperture in a metallic screen were published (Bethe, 1944; Bouwkamp, 1950a,b), followed recently by numerical simulations on NSOM probe models (Novotny *et al.*, 1995, and references therein). Comparing these results with experimental data has only rarely been accomplished (Betzig & Chichester, 1993) because of the bad quality of most NSOM probes. However, the quality of the FIB-modified NSOM probes that we have developed is such that we observe the single molecule patterns of Fig. 3 routinely for every probe (Veerman *et al.*, 1998). We used the expressions of Bethe and Bouwkamp to calculate intensity patterns for comparison with our experimental data. Figure 4 depicts a set of such calculated patterns for a molecule located with different orientations at a distance of 15 nm from a 100 nm aperture. The incoming polarization direction is linear along the y direction. As in Fig. 3, colour-coding has been used corresponding to the azimuth orientation of the molecule. Large variations of the intensity pattern can be observed, from an elliptical shape for a molecule orientated in the sample plane along the excitation polarization direction, to a set of two arcs for a molecule orientated perpendicular to the sample plane. These calculated patterns closely resemble the experimental data we obtain with FIB-modified probes. Three sequential NSOM fluorescence images are shown in Fig. 5(a–c) to demonstrate the similarity. The images were obtained with the 70 nm probe of Fig. 1(a) on the same sample as in Fig. 3. The direction of the far-field polarization (and thus the electric near-field distribution of the probe) was different for each image. It can be clearly seen that the intensity pattern of the molecules changes accordingly. We believe that these measurements show for the first time in such detail the optical near-field distribution of a NSOM probe with molecular spatial resolution.

To the best of our knowledge, the measurements described in this paper have an unprecedented optical resolution. The fluorescence contrast we observe is purely optical in nature. Due to the absence of height differences on the sample the contrast is not influenced by height artefacts (Hecht *et al.*, 1997). Figure 6 depicts a cross-section along the indicated vertical line in Fig. 5(c). The FWHM of the peaks is 45 nm, which is a value considerably smaller than the aperture size (70 nm). It is known that the higher the sharpness of the rims of the aperture, the higher the gradients of the electric field, the more

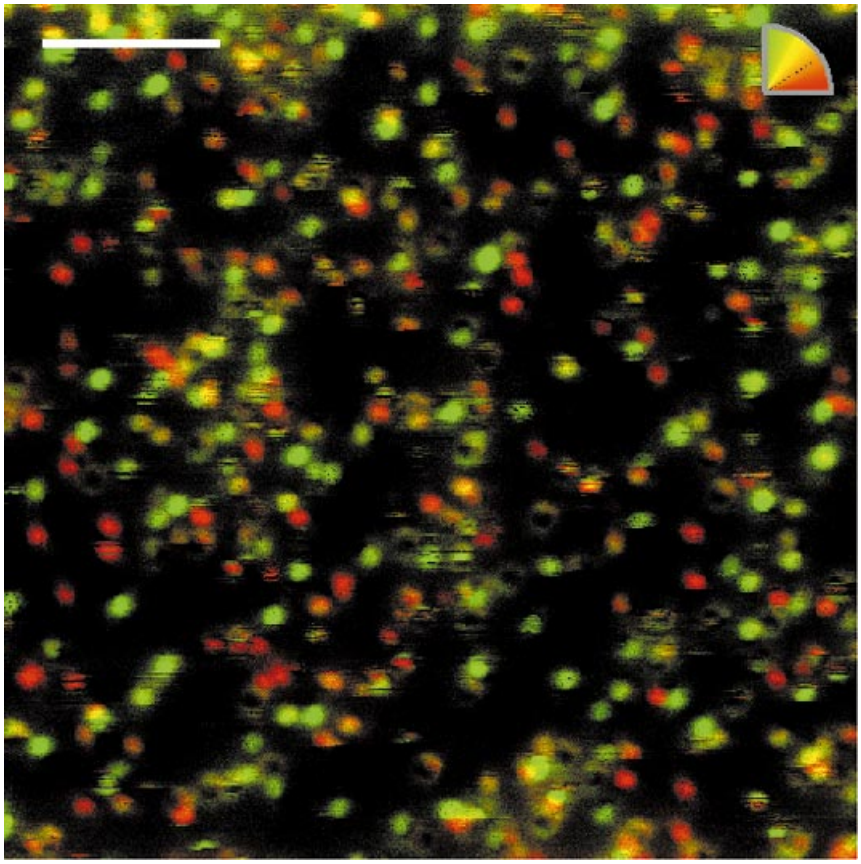

Fig. 3. NSOM fluorescence image ($4{\cdot}8 \times 4{\cdot}8\ \mu$m) obtained with the 70 nm aperture probe of Figure 1(a), showing single $DiIC_{18}$ molecules embedded in a 10-nm thin film of PMMA. Circularly polarised excitation light was used (as measured in the far field). A false-colour scale is used (see inset in upper right corner) which indicates the polarization direction of the fluorescence, and thus the orientation in the plane of the sample of the emission dipole moment of the molecules. The colour scale ranges from green (for molecules orientated along the vertical image direction) via yellow to red (for molecules orientated in the horizontal image direction). The molecules exhibit different shapes in the image, which is caused by an overlap of the absorption dipole moment with different polarization components of the optical field of the probe for different orientations of the absorption dipole moment. Bar = 1 μm.

pronounced the near-field intensity patterns (Bethe, 1944; Bouwkamp, 1950a,b; Novotny *et al.*, 1995). Furthermore, with increasing distance from the probe the fields expand and the obtainable resolution decreases. Thus, the effective resolution we measure is determined both by the sharpness of the aperture rim (ultimately limited by the $\approx 6{\cdot}5$ nm optical penetration depth for aluminium) and the distance between molecule and probe (≈ 15 nm).

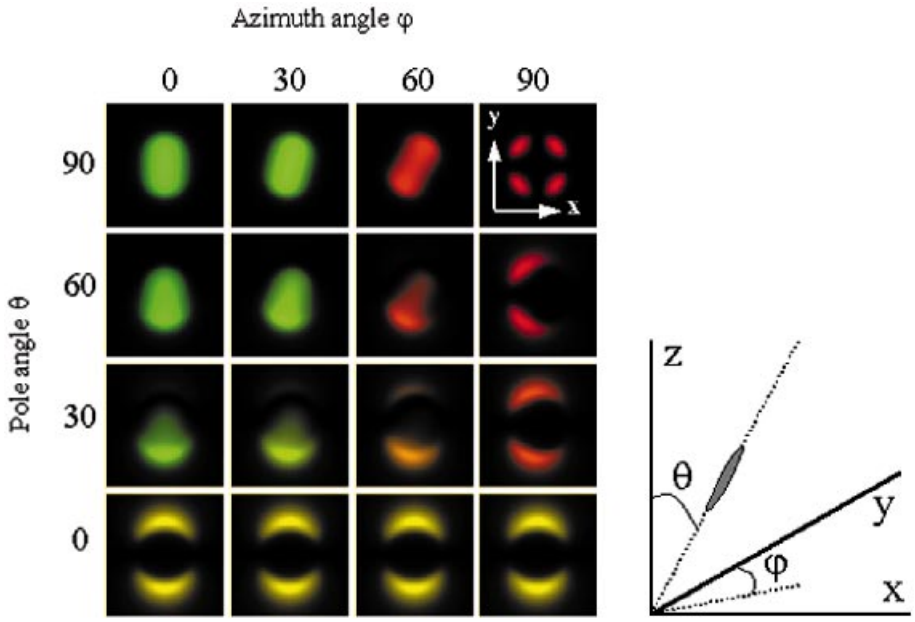

Fig. 4. Calculated intensity patterns for a single molecule at different orientations at a distance of 15 nm from a 100-nm aperture. Each image represents an area of 200×200 nm. The azimuth angle is in the plane of the aperture relative to the polarization direction, and the pole angle is relative to the aperture plane normal. The incoming polarization is linear along the *y* direction. Colour-coding as in Fig. 3 is used to indicate the azimuth orientation of the molecules. Every image has been normalized to its maximum intensity value.

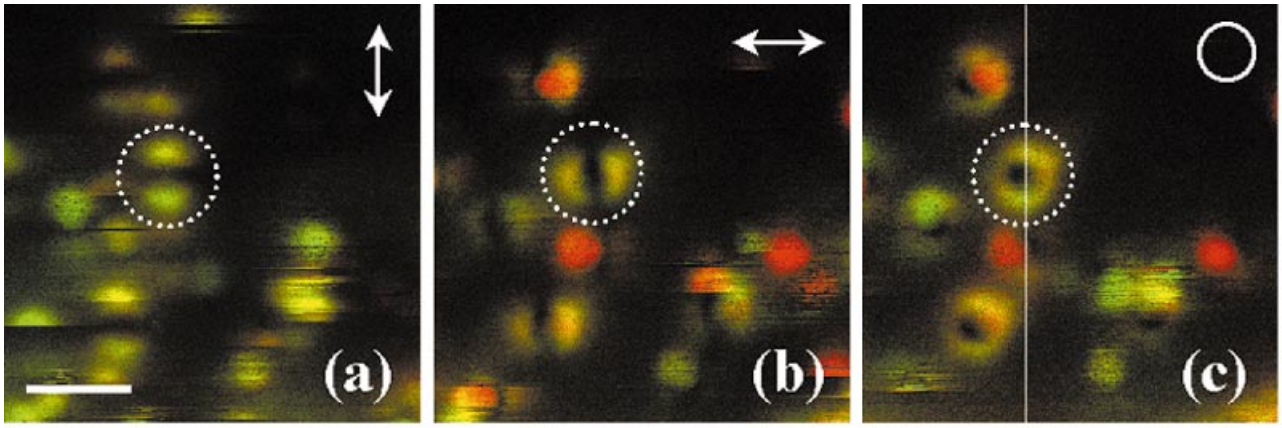

Fig. 5. Series of three successive NSOM fluorescence images of the same area ($1{\cdot}2 \times 1{\cdot}2\ \mu$m) of a sample of $DiIC_{18}$ molecules embedded in a 10-nm thin film of PMMA, measured with the 70 nm aperture probe of Fig. 1(a). The excitation polarization (as measured in the far field) was changed between linear in the vertical image direction (a), linear in the horizontal image direction (b), and circular (c). The appearance of the molecules changes accordingly as, for example, for the molecule in the dashed circle that is orientated perpendicular to the sample plane. Bar = 300 nm.

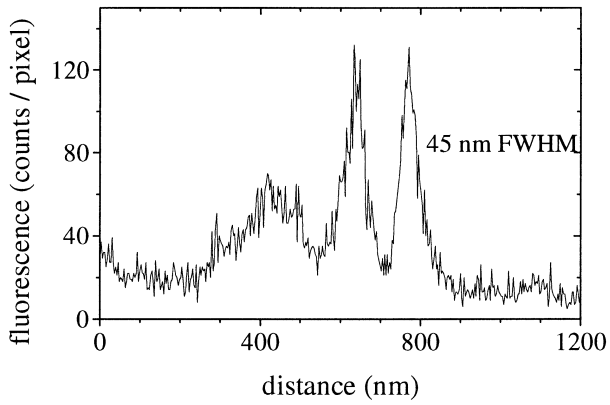

Fig. 6. Cross-section through one of the ring-like molecules in the right image of Fig. 4 (as indicated by the line) showing a FWHM optical resolution of 45 nm. This resolution is determined by the sharpness of the edge of the aperture, rather than by the aperture size itself (70 nm).

An unexpected result in the images of Figs 3 and 5 are the colour differences (indicating polarization of the emitted light) within the intensity pattern of a single molecule. For a fixed orientation of the molecule, a fixed polarization is expected (as in Fig. 4). However, we observe an alteration of the emission polarization depending on the relative position of the molecule with respect to the probe. We are currently investigating this effect, which is probably caused by distortion of the dipole radiation pattern by the probe.

Finally, another subject of current research is the relative intensity between the signals for different molecules. The calculated images in Fig. 4 were all normalized to equalize the peak intensities, but in reality the peak intensities of the patterns vary by approximately two orders of magnitude. We are working on combining the relative peak intensity differences measured (i.e. between the circular and ring-like patterns) with adequate models for the dipole radiation patterns.

In conclusion, we have developed new FIB-modified NSOM probes of high quality, as illustrated by the measurements described in this paper. The results demonstrate the potential of NSOM to obtain optical information with unsurpassed subwavelength resolution.

Acknowledgements

We thank Bert Otter for his assistance with the FIB machine. This work is financially supported by the Stichting voor Fundamenteel Onderzoek der Materie (FOM).

References

Bethe, H.A. (1944) Theory of diffraction by small holes. *Phys. Rev.* **66,** 163–182.

Betzig, E. & Chichester, R. (1993) Single molecules observed by near-field scanning optical microscopy. *Science*, **262,** 1422–1425.

Bouwkamp, C.J. (1950a) On Bethe's theory of diffraction by small holes. *Philips Res. Report*, **5,** 321–332.

Bouwkamp, C.J. (1950b) On the diffraction of electromagnetic waves by small circular disks and holes. *Philips Res. Report*, **5,** 401–422.

Hecht, B., Bielefeldt, H., Inouye, Y., Pohl, D.W. & Novotny, L. (1997) Facts and artifacts in near-field optical microscopy. *J. Appl. Phys.* **81,** 2492–2498.

Hollars, C.W. & Dunn, R.C. (1998) Evaluation of thermal evaporation conditions used in coating aluminium fiber-optic probes. *Rev. Sci. Instr.* **69,** 1747–1752.

Karrai, K. & Grober, R.D. (1995) Piezoelectric tip-sample distance control for near field optical microscopes. *Appl. Phys. Lett.* **66,** 1842–1844.

Novotny, L., Pohl, D.W. & Hecht, B. (1995) Scanning near-field optical probe with ultrasmall spot size. *Opt. Lett.* **20,** 970–972.

Ruiter, A.G.T., Veerman, J.A., Garcia-Parajo, M.F. & van Hulst, N.F. (1997b) Single molecule rotational and translational diffusion observed by near-field scanning optical microscopy. *J. Phys. Chem. A*, **101,** 7318–7323.

Ruiter, A.G.T., Veerman, J.A., van der Werf, K.O. & van Hulst, N.F. (1997a) Dynamic behavior of tuning fork shear-force feedback. *Appl. Phys. Lett*. **71,** 28–30.

Veerman, J.A., Otter, A.M., Kuipers, L. & van Hulst, N.F. (1998) High definition aperture probes for near-field optical microscopy fabricated by focused ion beam milling. *Appl. Phys. Lett*. **72,** 3115–3117.